High Yield of Triplet Generation Via Intramolecular Singlet Exciton Fission in a Quinoidal Bithiophene

9 AUTHORS, INCLUDING:

Juan Aragó
The University of Warwick
33 PUBLICATIONS **160** CITATIONS

SEE PROFILE

Juan J. Serrano-Perez
Universidad Europea de Valencia
25 PUBLICATIONS **261** CITATIONS

SEE PROFILE

Juan Teodomiro López Navarrete
University of Malaga
334 PUBLICATIONS **5,227** CITATIONS

SEE PROFILE

Juan Casado
University of Malaga
226 PUBLICATIONS **3,679** CITATIONS

SEE PROFILE

High Yield Ultrafast Intramolecular Singlet Exciton Fission in a Quinoidal Bithiophene

Oleg Varnavski,[†] Neranga Abeyasinghe,[†] Juan Aragó,[‡] Juan J. Serrano-Pérez,[‡] Enrique Ortí,[‡] Juan T. López Navarrete,[§] Kazuo Takimiya,[||] David Casanova,[⊥,∇,¶] Juan Casado,*[,§] and Theodore Goodson, III*[,†]

[†]Department of Chemistry, University of Michigan, Ann Arbor, Michigan 48109, United States
[‡]Instituto de Ciencia Molecular, Universidad de Valencia, 46980 Paterna, Spain
[§]Department of Physical Chemistry, University of Malaga, 29071 Malaga, Spain
[||]Department of Applied Chemistry, Graduate School of Engineering, Hiroshima University, Higashi-Hiroshima 739-8527, Japan
[⊥]IKERBASQUE, Basque Foundation for Science, 48011 Bilbao, Spain
[∇]Kimika Fakultatea, Euskal Herriko Unibertsitatea (UPV/EHU), P.K. 1072, 20080 Donostia, Spain
[¶]Donostia International Physics Center (DIPC), 20018 Donostia, Spain

S *Supporting Information*

ABSTRACT: We report the process of singlet exciton fission with high-yield upon photoexcitation of a quinoidal thiophene molecule. Efficient ultrafast triplet photogeneration and its yield are determined by photoinduced triplet−triplet absorption, flash photolysis triplet lifetime measurements, as well as by femtosecond time-resolved transient absorption and fluorescence methods. These experiments show that optically excited quinoidal bithiophene molecule undergoes ultrafast formation of the triplet-like state with the lifetime ~57 μs. CASPT2 and RAS-SF calculations have been performed to support the experimental findings. To date, high singlet fission rates have been reported for crystalline and polycrystalline materials, whereas for covalently linked dimers and small oligomers it was found to be relatively small. In this contribution, we show an unprecedented quantum yield of intramolecular singlet exciton fission of ~180% for a quinoidal bithiophene system.
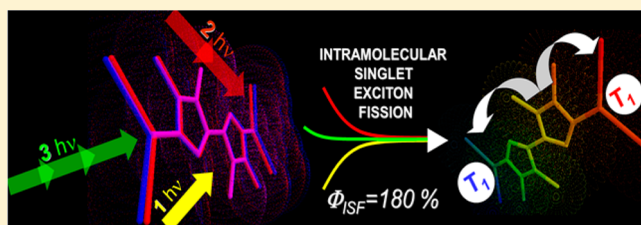
S inglet exciton fission (SEF), discovered almost 50 years ago, has recently attracted renewed interest due to potential applications.[1−3] SEF, in which two triplet excited states are created from one singlet excited state, can potentially provide a pathway to increase the energy conversion efficiency in organic solar cells if each of the two generated triplet states is able to inject an electron.[2−7] SEF has been found in a number of selected systems, including large polyacenes,[8,9] polymers[10−12] carotenoids,[13−15] and in covalent dimers.[16−18] Although the list of compounds that have been shown to undergo SEF continues to grow, a high-yield multielectron generating system for real photovoltaic applications remains to be found.

SEF is a quantum-mechanically allowed process as opposed to the spin-forbidden singlet−triplet transition (intersystem crossing). Under favorable $E(S_1) > 2E(T_1)$ energetics, the fission process can be very fast due to its spin-allowed nature.[1,3,6,7] In most of the known SEF materials for photovoltaics, the correlated triplet pair state $^1(T_1T_1)$ is formed by sharing the initial singlet monomer exciton energy with a neighboring molecule giving rise to an intermolecular excimer state in which each molecule embodies a triplet and the two

triplets are electronically coupled to form a correlated triplet pair with singlet multiplicity $^1(T_1T_1)$. Even in the assumption of favorable energetics, the single-molecule excitation in these systems evolves to a bimolecular excimer, a process that might be a quite limiting step due to the intermolecular nature of $^1(T_1T_1)$ that requires suitable intermolecular electronic coupling (adequate π−π contact and molecular orientation).[6,7]

Intramolecular SEF quantum yields reported until very recently[12] were small, typically well below 30%, whereas for polycrystalline solids made from the same chromophores, the intermolecular SEF yield could reach 200%.[6,16,18] The reason for this was not clearly understood and the potential of intramolecular fission has not been fully explored.[6,18] In an exciting new development, high efficiency intramolecular SEF has been recently demonstrated in donor−acceptor polymers.[12] Intramolecular SEF is a very attractive route for multiple charge generation as it allows for accurate tuning of the geometry and intramolecular interactions through chemical synthesis. As a
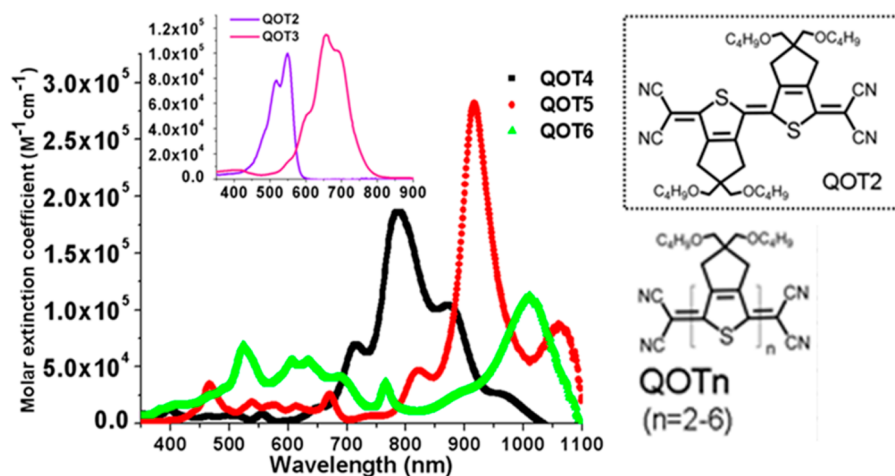
Figure 1. Steady-state absorption spectra for QOTn oligomers indicating their broader reach of the visible and near-infrared wavelengths. The structure of quinoidal bithiophene QOT2 investigated in this work.

molecular property, SEF itself in this case may not require long molecular ordering or fine adjustment of intermolecular interaction in a not-so-easily controllable assembling process. Additionally, for intramolecular SEF molecules, we can control the D−A interface parameters for charge separation much more precisely as compared to the microcrystalline contact, for example, by bonding the SEF molecule to a charge separation unit.

Besides covalent dimers, intramolecular SEF is known to occur in particular carotenoids bound to photosynthetic antenna light-harvesting proteins.[13,14] It also has been found in conjugated polymers.[10−12] The possibility of efficient localization of the resulting triplets in well-separated polymer fragments within the maximal conjugation length plays an important role in generation of separated triplets. From this perspective, a large molecular weight disordered polymer can be considered as multi-segment system showing some features of intermolecular process even in diluted solution (e.g. self-chain crossings due to disorder). From a mechanistic perspective, the polymer resorts to distance the two triplet excitations via extended conjugation length and delocalization of a parent singlet, whereas the small molecule may mostly use a conformational gateway to accommodate them. In an attempt to better understand the SEF process in small molecules, dimers formed by two active molecules covalently connected by electronically inactive units have been studied.[16−18] These are certainly unimolecular entities, but they do not directly imply the concept described in carotenoids and conjugated polymers. In fact, these weakly coupled dimers show very low SEF quantum yields and, more importantly, a slow and non-competitive triplet formation rate.[18] On the other hand, conjugated polymers with strongly coupled charge-transfer character units demonstrated high SEF efficiency up to 170%.[12]

It is well known that absorption processes can efficiently promote the direct generation of multiple carriers in inorganic semiconductors and carbon nanotubes.[19] However, in organic molecules, these multiexciton states can be strongly coupled and double electron injection capability is questionable. The molecular system should allow for two triplet excitations being more or less independent, but quantitatively, the extent of this anticipated independence with respect to efficient double electron injection remains unclear. For example, Chan et al. have demonstrated that the charge transfer rate from the

correlated pair intermediate state of pentacene (ME/ME′) to C_{60} is higher than that from separated triplets and, more importantly, that both electrons are transferred.[3] This observation indicates the importance of the intermediate state $^1(T_1T_1)$ for multiple charge extraction process and that the formation of perfectly independent triplet states may not be essential for efficient double charge injection.

Although creation of the efficient photovoltaic cell utilizing SEF to exceed Shockley−Quiesser limit goes beyond SEF suggesting the use of additional red-absorbing species to prevent the drop in open circuit voltage,[2] the discovery of new organic molecules possessing efficient intramolecular SEF in relatively small molecules and oligomers is an important step toward potentially controlling the SEF efficiency via chemical synthesis that will be pivotal for next generation photovoltaic applications. Efficient intramolecular SEF system in comparison with the intermolecular SEF counterpart can give the following important benefits: (i) a higher efficiency (intermolecular steps preceding triplet−triplet formation are made unnecessary), (ii) the SEF−active molecule can be potentially bound to the electron acceptor with a minimal travel distance for triplet exciton to reach the acceptor, thus ensuring more efficient electron injection competitive to detrimental triplet−triplet annihilation process, and (iii) the system efficiency is expected to be less susceptible to the defects like those associated with the imperfections in microcrystalline structures.

Tetracyanomethylene quinoidal oligothiophenes (QOTn, Figure 1) have recently attracted substantial attention due to their unusual linear and nonlinear optical properties.[20−27] Long quinoidal oligothiophenes have been shown to possess a biradicaloid character in their ground state.[23−28] Biradicaloids are known to have low-lying triplet energy levels and therefore are promising structures to meet the requirement $E(S_1) \geq 2E(T_1)$.[6,7,29,30] The quinoidal structure of the thiophene rings results in a mostly planar ground state molecular configuration that undergoes distortions and twisting to stabilize their excited state.[24] Moreover, QOTn molecules are equipped with terminal −CN acceptor groups that may serve to facilitate the efficient formation of the correlated triplet pair state and subsequent separation into two individual triplets.[31,32] The quinoidal features, together with the great photostability of quinoidal thiophenes, make QOTn very promising candidates for a new
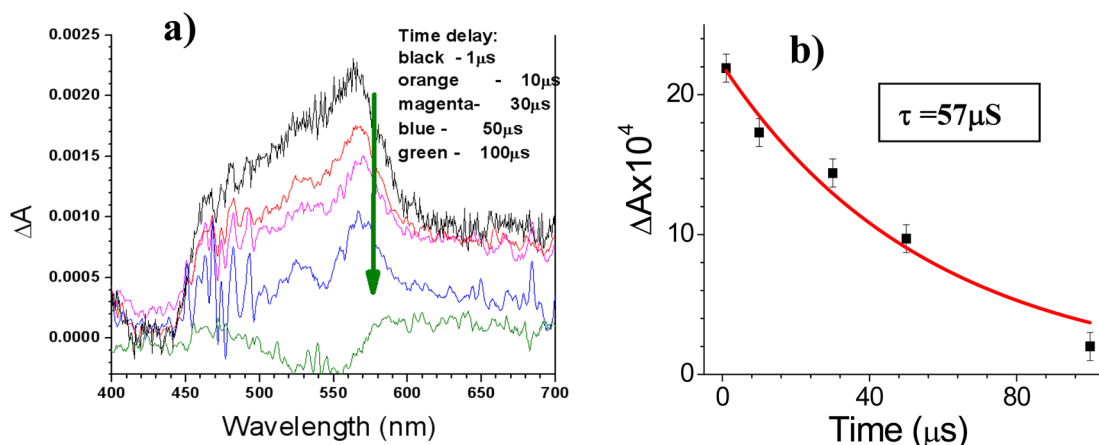
Figure 2. Efficient generation of long-lived species. (a) Transient absorption spectra (flash photolysis) of QOT2 at 445 nm excitation that yields 57 μs-lived transient species. (b) Fitting of the 570 nm excited state absorption to the exponential decay function.
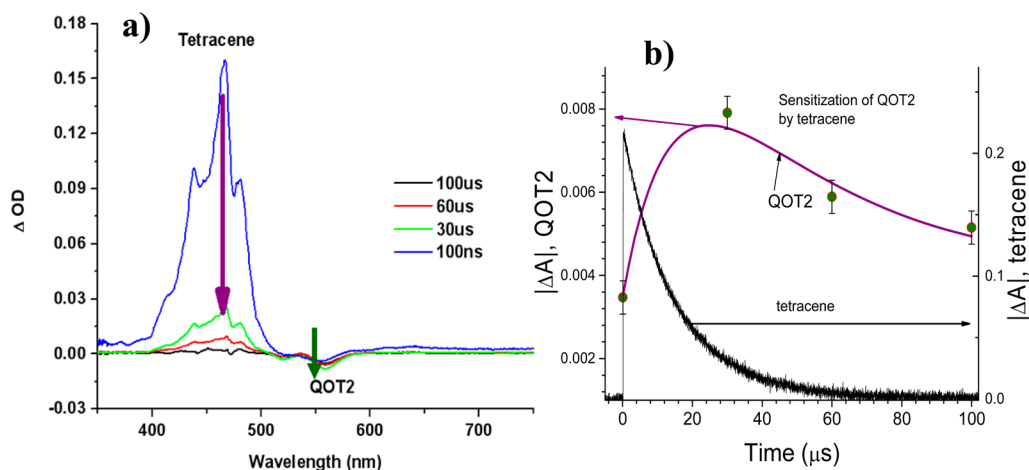

Figure 3. (a) Transient absorption spectra of tetracene and QOT2 sensitized with tetracene at excitation of 470 nm. (b) Triplet energy transfer kinetics from tetracene to QOT2 derived from transient absorption spectra. Tetracene quenching kinetics is also shown.

generation of organic molecules for photovoltaics by virtue of the intramolecular SEF process.

In this paper, we report on the generation of ∼180% yield of triplet excitons via intramolecular SEF in a relatively small molecule tetracyanoquinodimethane bithiophene (QOT2, Figure 1). QOT2 displays favorable energetic conditions for SEF imparted by its pro-biradicaloid character. We show that QOT2 undergoes ultrafast formation of a triplet-like species that lives for at least 57 μs using femtosecond and microsecond transient absorption measurements, ultrafast nonlinear transmission, time-correlated single photon counting, and femtosecond time-resolved fluorescence measurements. Moreover, our multiconfigurational CASSCF/CASPT2 and RAS Spin-Flip (SF) quantum chemical calculations on QOT2 confirm the possibility of intramolecular SEF by outlining the general energetic landscape during the formation of triplets. Using both experiment and theory we describe the pertinent mechanisms yielding the high population of the multiexciton state under impulsive conditions, which efficiently produces triplet excitons via intramolecular SEF. We demonstrate that QOT2 has all the ingredients necessary to be utilized in highly efficient organic photovoltaic devices operating via intramolecular SEF. Investigations on QOTn have revealed that their steady-state absorption spectra extend much farther to the red as compared to the corresponding aromatic oligomers (Figure 1).[22,25,33]

Moreover, these quinoidal structures have shown biradicaloid character of the ground state indicating the presence of low-lying triplet states that can help to meet the energetic requirement for singlet exciton fission $[2E(T_1) < E(S_1)]$.[24,30] Experiments have been performed in QOT2 solutions having concentration in the range 2×10^{-6} M to 10^{-3} M (depending on the experiment), thus making the intermolecular processes very improbable on the time scales of the experiments.[34] No concentration dependence of the steady-state spectra as well as the kinetics have been detected in this concentration range indicating negligible aggregate formation.

In order to establish the formation of triplet species, we have conducted transient absorption experiments on QOT2 excited at 445 nm using a flash photolysis apparatus as well as sensitization of the QOT2 triplets using tetracene. The excited state absorption (ESA) detected for the directly photo-generated species (Figure 2) displayed a peak at ∼570 nm and had a lifetime of 57 ± 6 μs. This long lifetime taken together with the absence of systematic solvent polarity and viscosity dependence as well as the presence of magnetic field effects (see Supporting Information) strongly suggest the formation of a triplet (or higher multiplicity) species upon photoexcitation of QOT2.

Using the same setup we have also observed a tetracene-sensitized transient absorption feature associated with the

triplet exciton energy transfer from the tetracene to QOT2 (Figure 3, Supporting Information Figures S1 and S2). Interestingly, in contrast to the direct excitation, sensitized QOT2 showed ESA shifted to the red (~600 nm) as compared to that for the direct excitation with a measured lifetime of 111 ± 19 μs (well beyond the tetracene triplet lifetime of 38 μs; Figure 3, Supporting Information Figure S1). The shortening of the tetracene lifetime to 14.9 ± 0.1 μs clearly indicates the triplet sensitization of QOT2 by tetracene.

We can establish two possible long-lived transient species for photoexcited QOT2:

1. Single triplet species that lives for 111 μs, from the sensitization experiment.

2. A long-lived species distinct from and that lives shorter than a single triplet exciton (57 μs), from the direct singlet excitation of the QOT2.

It is clear from these experiments that the direct excitation of QOT2 forms a species that has non-singlet character and that shows somewhat different excited state properties in comparison with the single triplet exciton produced by sensitization route. We assign this species to the triplet pair residing on one QOT2 molecule. The observation of the triplet pair on direct excitation with a lifetime shorter than that for a single triplet exciton may indicate an enhanced contribution of the triplet–triplet annihilation process if more than one triplet, that is, a triplet pair, is formed in one molecule under direct excitation. It is also possible that the molecular conformation that stabilizes a triplet pair on one molecule is somewhat different from that stabilizing the single triplet, which can result in different associated decay rates. Also, having an excited triplet pair distinguishable from the single triplet exciton (111 μs lifetime) is an indirect indication that the 57 μs-lived species has derived from a process other than intersystem crossing. This experiment has also located the triplet state energy of the QOT2 to be below triplet energy of tetracene, that is, 0.98 eV thus confirming the favorable energetics $E(S_1) > 2E(T_1)$ for SEF in QOT2 ($E(S) \cong 2.26$ eV).

We have examined the excited state absorption of QOT2 at 890 nm under excitation with a femtosecond pulse train at 445 nm. The 890 nm probe beam has been produced by the femtosecond laser system delivering 130 fs pulses at a repetition rate of 80 MHz, whereas its second harmonic (445 nm, 2.79 eV) has been used as a pump. The 445 nm pump pulse train excites high-lying vibronic states of the one-photon-allowed transition (high energy side of the band spreading from 400 to 600 nm in Figure 1). In this experiment, a small fraction (<1 mW) of the fundamental beam (890 nm) probes the transmission of the sample in the wavelength range where the linear absorption of the sample is negligible. A surprisingly strong drop in transmission was observed at 890 nm (Figure 4).

Almost complete attenuation of the 890 nm probe beam under the moderate pump at 445 nm (~14 mW) detected in this experiment is due to accumulation of a significant number density of excited state absorbing species. In order to better characterize this absorbing species, we performed this transmission experiment for QOT2 dissolved in a variety of solvents possessing different polarities and viscosities. Figure 5 shows the probe transmission profiles for QOT2 in solvents of different polarities ranging from nonpolar cyclohexane to highly polar acetonitrile. It is seen that the transient absorption induced by the 445 nm beam does not have systematic polarity dependence ruling out the formation of long-lived charge
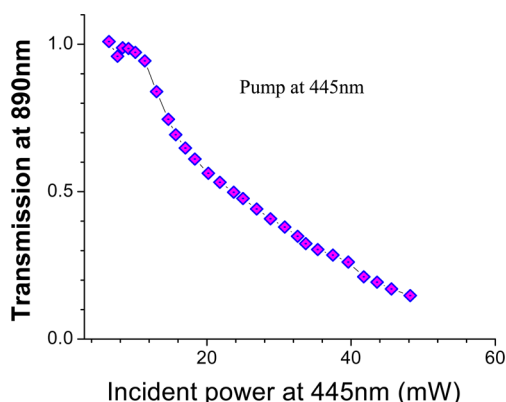

Figure 4. Transmission of QOT2 for the probe light at 890 nm as a function of the pump power at 445 nm.
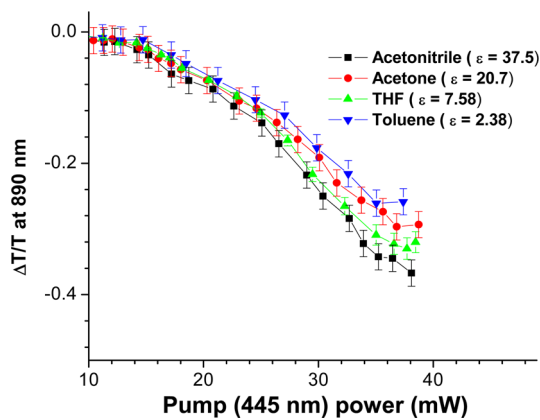

Figure 5. Transmission of QOT2 for the probe light at 890 nm as a function of the pump power at 445 nm in solvents of different polarity.

transfer products sensitive to the polar environment (such as radical anions and cations). The induced absorption profile also did not show measurable dependence on the solvent viscosity (Supporting Information Figure S3) thus making the contribution of long–lived conformers or excited state species created in intermolecular processes controlled by diffusion (e.g. excimers) very improbable.

From the induced triplet absorption shown in Figure 4, one can estimate the number density of accumulated triplet excited states n_{TE} that is necessary to produce the observed beam attenuation of 48.5% at 890 nm for the incident pump (445 nm) power of 14.5 mW. The molar extinction coefficient for triplet–triplet absorption was estimated to be 9.5×10^3 M^{-1} cm^{-1}: $n_{TE} = 3.65 \times 10^{16}$ triplets/cm^3. The number density of molecules in the singlet excited state n_S^* created by the 445 nm laser pulse can be easily estimated from the optical density of the sample and pulse energy: $n_S^* = 4.57 \times 10^{12}$ singlets/cm^3. Comparing the number of triplet states accumulated during the triplet lifetime with n_{TE}, the singlet–triplet conversion quantum efficiency α_{ST} can be calculated: $\alpha_{ST} = 1.76$ or 176% (see Supporting Information for details). In line with the unusually strong beam attenuation at 890 nm, the calculated singlet–triplet conversion efficiency above 100% indicates the presence of a very efficient SEF process in QOT2.

Previous studies on singlet exciton fission (tetracene, pentacene, carotenoids, etc.) have reported the identification of an intermediate correlated triplet-pair state.[3,5,13,35] This intermediate state was found to emerge almost simultaneously
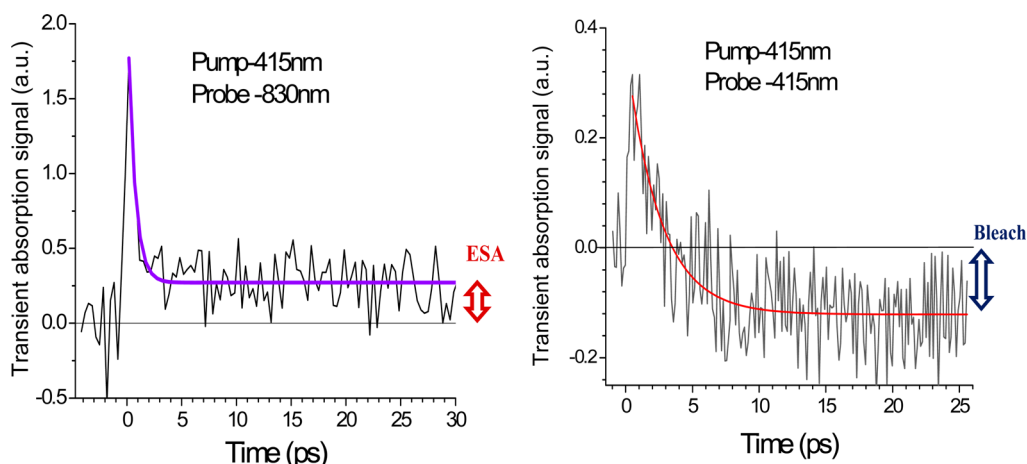
Figure 6. (a) Two-color pump–probe dynamics in the first 30 ps for QOT2 under 415 nm pump and 830 nm probe indicating the ultrafast formation (<1 ps) of the long-lived species (b) Degenerate pump–probe dynamics showing formation of long-lived ground state bleach.
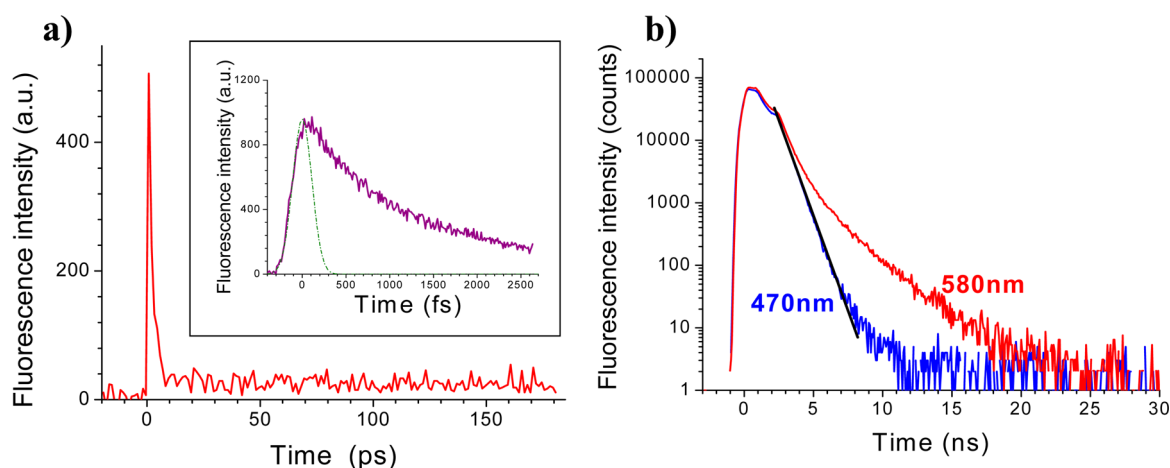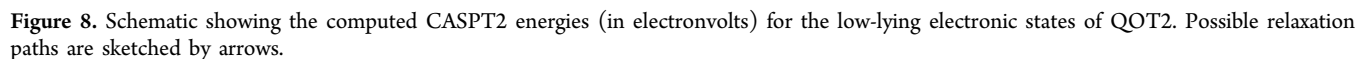

Figure 7. Time-resolved fluorescence dynamics. (a) Femtosecond time-resolved fluorescence decay at 600 nm. Inset: Short time scale fluorescence decay; instrument response function (fwhm = 0.25 ps) is indicated by dash-dot line. (b) Time-resolved fluorescence decay measured by time-correlated single photon counting (TCSPC) at 470 and 580 nm emission wavelengths.

(within the ~first picosecond) with the formation of a singlet excited state.[3,35] Moreover, it was found that this ultrafast formation is directly assisting SEF to compete with other radiative and nonradiative relaxation processes to achieve highly efficient triplet generation.[6] In order to investigate possible ultrafast origins of the triplet-like excitons (triplet pair or correlated triplet pair), we have carried out femtosecond time-resolved two-color pump–probe experiments on QOT2 using a low-noise, cavity-dumped Ti-sapphire femtosecond oscillator. The excitation occurred at 415 nm, whereas the probe pulse wavelength was at 830 nm. The fast initial decay component (<1 ps) of the excited state absorption in Figure 6 is due to transient absorption contribution of a short-lived singlet excited state. This decay is followed by the excited state absorption by a long-lived species, which can be attributed to the absorption of the triplet-like species detected in the above experiments.

Although the exact rise time of the long-lived transient absorption is obscured by the fast singlet state decay, it is clear that the long-lived absorption is fully established after 1 ps. It can be inferred, then, that the same absorbing species is existent until 57 μs to give rise to the excited state absorption at 570 nm and at longer wavelengths (830 nm in this case). Moreover, a similar (~1 ps) decay profile was observed for our time-

resolved fluorescence experiment (see above) at 600 nm emission substantiating the ultrafast decay (~1 ps) of the initial singlet excitation. This surprisingly short build up time for the triplet-like state in the subpicosecond time range cannot be a result of the regular intersystem crossing induced by spin–orbit coupling mechanism as the latter is an orders-of-magnitude (10^{10} s^{-1} as opposed to $>10^{12}$ s^{-1}) slower process for systems without heavy atoms.

Out of the two interconverting singlet and triplet transient species generated on the picosecond time scale, the lowest singlet state population can be followed by the fluorescence dynamics. We have conducted femtosecond time-resolved fluorescence measurements to correlate the singlet state population dynamics with the triplet state population build up time. The time-resolved 600 nm (2.07 eV) fluorescence profile measured with the fluorescence upconversion setup is shown in Figure 7a. It is clearly seen that the fluorescence (thus, the singlet state population) decays within a few picoseconds. Best fit analysis of the short time-scale fluorescence dynamics (Figure 7a, inset) showed biexponential decay with time constants of 0.61 $\pm$ 0.1 ps and 2.0 $\pm$ 0.3 ps, which are in excellent agreement with the transient absorption experiment monitoring mostly singlet excited states.[20,21] This

Figure 8. Schematic showing the computed CASPT2 energies (in electronvolts) for the low-lying electronic states of QOT2. Possible relaxation paths are sketched by arrows.

decay time also correlates well with the triplet-like population build up time estimated from the transient absorption experiment monitoring the triplet excited state absorption (Figure 6). These experiments showed that ultrafast singlet−triplet transformation plays a dominant role in the singlet population decay. The observed fast transformation of the singlet states into the triplet-like states (<1 ps) clearly indicates an intramolecular SEF process as the intersystem crossing rate is expected to be orders of magnitude slower.[6]

We have also performed time-correlated single-photon counting (TCSPC) measurements of the fluorescence decay at different wavelengths in order to better probe any possible long-lived emission components (e.g., delayed fluorescence). For the fluorescence at 580 nm (2.14 eV) reflecting the population of the lowest emissive singlet state, we found a decay on the nanosecond time scale (Figure 7b) as opposed to the fast decay at 470 nm (2.64 eV) mainly following the instrument response function profile.

The 470 nm fluorescence signal monitors the population dynamics of a higher-lying singlet state. As the excitation intensity in this photon counting experiment was extremely low (*less than one excitation per 10 000 molecules*), the singlet−singlet annihilation (and charge recombination) can be readily excluded. The 580 nm fluorescence long tail is suggested to be due to the singlet excitations formed as a result of weak triplet−triplet exciton annihilation (delayed fluorescence). It decays well beyond the major excited singlet decay component of ∼2 ps for QOT2[20,21] (shown in Figures 6 and 7a). The presence of a long-lived nonexponential emission component related to the delayed fluorescence was often used as a strong indication of the triplet state population.[36−38] It is also worth noting that due to the low concentration of molecules in solution used in this experiment ($<10^{-5}$ M), annihilation of two triplet excitations residing on different molecules can be neglected and the observed delayed fluorescence might be associated with the presence of two triplets residing on one molecule. The delayed fluorescence, as detected with this setup, lasts shorter than the triplet-related transient absorption features (Figure 2). It can be associated with low signal-to-noise ratio of the setup to detect extremely weak (in part due to relatively low annihilation rate) delayed fluorescence tail. Some conformational inhomogeneity can be also contributing to the enhanced delayed fluorescence

at short times. It is also worth noting that the energy of the resultant singlet (following triplet−triplet annihilation) should be lower than 2.64 eV not to appear in the 470 nm emission. This distinction between the 470 and 580 nm emission may further indicate the excited-state energy relaxation of a correlated triplet-pair state (or an intermediate state) prior to their separation into two triplets. Additionally, we carried out magnetic field-dependent measurements to probe the triplet origin of the observed transients. We have conducted magnetic field measurements on the transmission drop and on the fluorescence. The excited state absorption at 890 nm increases by a value that is definitely beyond the noise uncertainty when an external magnetic field of ∼100 G is applied to the sample (Supporting Information, Figure S10). This observation indicates an increase in triplet-like population compared to the zero-field case. Because the observed excited state absorption corresponds to long time scales, it can be inferred that, by the point when ESA is significant, the triplet-like states have randomized their populations across the nine possible spin states[6,9] so that the pathways available for triplet−triplet annihilation are reduced. The magnetic field dependent fluorescence has been also observed. The data is shown in Supporting Information (Figures S11, S12, and S13). There is a clear change of the fluorescence intensity with and without the 100 G magnetic field. Although the detailed mechanism of these effects is still under investigation, these experiments demonstrating a magnetic field dependence of the photo-generated absorbance and fluorescence in QOT2 provide additional support to its spin multiplet origin.

Multiconfigurational CASPT2 quantum-chemical calculations have been performed to explore the electronic structure and excited states of the strongly electron correlated QOT2 system (Figure 8). The CASPT2 protocol has been shown to provide accurate descriptions of photophysical/photochemical processes.[39,40] Substituents at the β, β' positions of QOT2 have been omitted to simplify the model and reduce the computational cost. Calculations have been carried out using an active space of 10 electrons in 8 π molecular orbitals and the cc-pVDZ basis set (see Supporting Information for full computational details). Molecular geometries of both the ground and the excited electronic states have been optimized at the CASPT2 level.

CASPT2 calculations predict a strong one-photon-allowed vertical excitation to the 1^1B_u state at 2.06 eV, which correlates with the experimental band at 2.25 eV in the UV–vis absorption spectrum. This $1^1A_g \rightarrow 1^1B_u$ excitation is mainly described as a one-electron promotion from the $7a_u$ HOMO to the $7b_g$ LUMO (Supporting Information Figure S4). In the Franck–Condon region, the next 2^1A_g excited singlet state lies at 2.19 eV (0.13 eV higher than the 1^1B_u). This dipole-forbidden $1^1A_g \rightarrow 2^1A_g$ excitation mainly results from a double electron promotion revealing the multiexciton character of the 2^1A_g state.

We have also explored the minimum-energy regions for the two low-lying singlet excited states (1^1B_u and 2^1A_g). At the minimum of the 1^1B_u state, the 2^1A_g state lies 0.06 eV below and the energy difference increases to 0.31 eV at the optimized 2^1A_g geometry. These results clearly indicate that (i) the energy ordering of the two lowest-lying excited states (1^1B_u and 2^1A_g) is inverted when passing from the Franck–Condon region of the ground state $[1^1A_g \ (S_0) < 1^1B_u \ (S_1) < 2^1A_g \ (S_2)]$ to the minimum of the 2^1A_g state $[1^1A_g \ (S_0) < 2^1A_g \ (S_1) < 1^1B_u \ (S_2)]$ and (ii) the energy difference for a possible $1^1B_u \rightarrow 2^1A_g$ internal conversion is small (0.06 eV at the minimum of 1^1B_u) conforming with the ultrafast internal conversion between the 1^1B_u and the 2^1A_g states experimentally detected by Kobayashi et al.[20] At the CASPT2 optimized geometry of 2^1A_g, the vertical energy difference between the 2^1A_g and 1^1A_g states is computed to be 1.65 eV.

The low-lying triplet excited states were also calculated at the fully relaxed CASPT2 geometry of the 1^1A_g state (Supporting Information Figure S5). The first triplet excited state (1^3B_u) is predicted at 0.60 eV above the 1^1A_g ground state which is in qualitative agreement with the efficient QOT2 sensitization by tetracene described above. Although the relevant triplet species detected in the intramolecular SEF mechanism are multi-excitations, the evaluation of single molecule triplet excitations, relative to the relevant singlets, can provide a qualitative estimation as for the overall energetics of the SEF process. In this sense, the sum of the calculated energies of two isolated triplets residing on different molecules at the vertical states (i.e., $2 \times T_1 = 1.20$ eV) is lower than 1.65 eV (2^1A_g), thus anticipating a clear exoergic energy balance for a hypothetical intermolecular SEF process to take place. Two triplets stabilized on one molecule may have different total energy due to their close proximity and different stabilizing nuclear arrangement in comparison to that of two single triplets on two different molecules. Direct excitation flash photolysis and tetracene sensitization experiments indicated differences in spectra and kinetics. Nonetheless, ultrafast and efficient intramolecular triplet formation clearly shows that energetics remain favorable for the intramolecular case too. At the minimum of the 1^3B_u state (Supporting Information Figure S5), we have calculated the lowest-lying triplet excited states at CASPT2 and found that the lowest-energy $1^3B_u \ (T_1) \rightarrow 1^3A_g$ (T_2) triplet–triplet excitation has an energy of 1.80 eV with a relatively weak oscillator strength (0.084), whereas the most intense triplet–triplet excitation is associated with the $1^3B_u(T_1) \rightarrow 3^3A_g(T_6)$ transition with an energy of 2.82 eV and an oscillator strength of 0.605.

In polyenes, the 2^1A_g multiexciton singlet excited state (i.e., named covalent state) is described as a spin-wave state that consists of spin flip excitations.[41,42] For medium size polyenes, or carotenoids, the 2^1A_g is described as two intraethylene triplet excitations which are coupled into an overall singlet, or

$^1(T_1T_1)$. The electronic structure computed for QOT2 shows a definitive resemblance with that of polyenes and its 2^1A_g excitation can be viewed as a double triplet excitation or with a strong $^1(T_1T_1)$ component (see next section for spin flip calculations). Described the 2^1A_g excited state of QOT2 as a $^1(T_1T_1)$ excitation, we notice that the fully relaxed geometry of the 2^1A_g state features a significant elongation of the terminal carbon–carbon bonds by 0.096 Å (the central bond changes by 0.052 Å, see Supporting Information Table S1 and Figure S6) highlighting that the two coupled excitations are put apart toward the dicyanomethylene groups.

Restricted active space spin flip (RAS-SF) quantum chemical calculations reproduce with acceptable accuracy the relative energies of excited states of different multiplicity at a moderate computational cost.[43,44] RAS-SF calculations are thus very suitable to scan the energies of the excited states involved in SEF as it has been already described in a number of examples.[45−47] All calculations have been done with the double spin flip version of RAS-SF (RAS-2SF) using the lowest ROHF quintet determinant as the reference configuration and the same active space (10, 8) and basis set (cc-pVDZ) as used in the CASPT2 case.

It is presumed by many authors that the intramolecular SEF might be assisted by a high spin quintet (Q_1) molecular state which should mediate the full separation of the initial excitation into two independent intramolecularly comprised triplets.[6] RAS-2SF/cc-pVDZ calculations predict the low lying Q_1 state in QOT2 (1^5A_g) at more than 4.5 eV above the 1^1A_g ground electronic state (Supporting Information Figure S7). Because intramolecular SEF in carotenenoid-like molecules is accompanied by stabilizing molecular distortions,[13,14] we have scanned the energy evolution of the $2^1A_g/1^5A_g$ states by rotating from 0 to 90° around the central CC bond (bond 1 in Supporting Information Table S1) resulting in an overall destabilization of both states (Supporting Information Figure S7), which is unfavorable for any photophysical process taking place at moderately low energies as those observed here.

Anticipated by the structure of the 2^1A_g state described at the CASPT2 level above, we have explored the energy evolution of the relevant low-energy lying excited states with respect to the simultaneous rotation around the bonds linking the dicyanomethylene groups and the thiophenes in Supporting Information Figure S8 (bonds 5 and equivalent in Supporting Information Table S1). Interestingly, the sole state that is stabilized with this distortion is the 1^5A_g state, whereas the 2^1A_g gets destabilized being degenerate with the 1^5A_g at 90° conformation; this highlights the intrinsic multiradical nature of the multiexciton 2^1A_g of QOT2. We have calculated the tetraradical character of the 2^1A_g wave function as a function of the discussed rotation and found that it progressively increases, having a 100% tetraradical feature at 90° (Supporting Information Figure S9). One can argue that the biradical centers are spatially localized mainly at the terminal dicyanomethylene groups at this perpendicular disposition. This theoretical data reveals that a mechanism for intramolecular SEF in QOT2 assisted by a quintet state is rather unviable, as this requires high excitation energies to be activated. At the same time, the fact that distortions in the peripheral dicyanomethylene groups stabilizing the multiradical character alludes to a possible mechanistic pathway for intramolecular SEF with a twisted conformation of QOT2.

The theoretical description is in agreement with ultrafast spectroscopic results in QOT2. In our transmission experi-

ments with the 445 nm (2.79 eV) laser excitation, QOT2 is directly excited to high-energy vibrational levels of the one-photon allowed 1^1B_u (S_2) state predicted at 2.06 eV, which might relax to its minimum undergoing ultrafast internal conversion to the 2^1A_g (S_1) state. The inversion of the energy ordering of the two lowest-lying excited states during the relaxation process can lead to the adiabatic relaxation pathway associated with the avoided crossing. This description is similar to that proposed for intermolecular SEF in tetracene films, which describes an adiabatic pathway from 1^1B_u to an intermediate or "dull" state (could be the 2^1A_g in our case).[48] However, in tetracene there is an intermolecular excimer state, whereas in QOT2, this state is of intramolecular nature. In QOT2, the stabilization is provoked by a planarity distortion around the external C—C bonds connecting the thiophenes and the dicyano groups. Two vibrational modes strongly coupled to the dark (S*) state of QOT2 reported in ref 49 (1466 cm^{-1} due to stretching of the external C≡C bonds and 446 cm^{-1} due to the out-of-plane ring or interring deformation[49]) may support the adiabatic evolution along the avoided crossing from 1^1B_u (S_2) to the dark state. The small predicted energy difference near minimum of the 1^1B_u state ~0.06 eV may also suggest the existence of a conical intersection between the two potential energy hypersurfaces. Both mechanisms should warrant ultraefficient/ultrafast internal conversion in accordance with the population within ~1 ps (see blue path in Figure 8) of the 2^1A_g lowest excited singlet. In order for efficient intramolecular singlet exciton fission to occur, excited singlet state $^1(T_1T_1)$ coupling has to be high enough. In light of recent findings by Busby[12] and co-workers and Zhu and co-workers,[31,32] the presence of electron-withdrawing cyano groups as acceptors can facilitate strong coupling between singlet and triplet pair via charge-transfer state. Similarly, in QOT2 the presence of terminal —CN groups can render charge transfer character in its excited state which may be beneficial for the rapid formation of the triplet-pair and, thus, high intramolecular SEF efficiency in QOT2. The triplet pair created from the 2^1A_g state might share structural characteristics with the 1^5A_g quintet (both are electronically decoupled triplet pairs, only differing in the sign and degree of the spin correlation). This analogy suggests that once this intermediate species is formed it could find a stabilization pathway by rotating around the inter-ring and dicyanothiophene dihedral angles (such as in the quintet by RAS-2SF calculations, Supporting Information Figure S9), a relaxation route that increases its tetraradical character (T_1T_1) favoring the full dissociation into two intramolecular independent triplets and enhancing the SEF efficiency up to values, 180%, close to complete singlet−triplet photoconversion of 200%. This distortion gateway of the correlated triplet pair is similarly suggested in carotenoid-like systems as the way to accommodate the two triplets.[13,14] These species are formed within picosecond time-scales and owing to its triplet character have a long lifetime of 57 μs in our case. The two intramolecular triplets or the intermediate correlated triplet pair $^1(T_1T_1)$ may follow the way back to the 2^1A_g singlet from which would weakly emit resulting in delayed fluorescence. Experimental observation of the delayed fluorescence at longer wavelengths (580 nm, 2.14 eV) rather than for the 470 nm (2.64 eV) indicates the upper level of the $^1(T_1T_1)$ energy, which is in line with calculated energy of 1.65 eV.

Given the two-photon absorption character of the $1^1A_g \rightarrow 2^1A_g$ transition, the dark state can be directly populated by two-photon excitation (see black path in Figure 8). We have previously reported that $1^1A_g \rightarrow 2^1A_g$ two-photon activity for QOT2 lead to relevant three-photon absorption (two-photon mediated three photon absorption), allowing the population of even higher energy excited states that would also relax down to the 2^1A_g (see maroon path in Figure 8).[21] We have observed the nonlinear absorption build-up associated with triplet generation under multiphoton excitation at 800 nm. Interestingly, the number density of excited singlet states producing specific induced absorption in this experiment was estimated to be very close to that created with one-photon excitation described above ($n_S^* = 4.57 \times 10^{12}$ singlets/cm^3). This result indicates the same mechanism and efficiency of triplet generation for both routes of singlet excitation.

Finally, the buildup of this strong triplet-like population is responsible for the drop in transmission for the 890 nm probe beam observed in the experiment. A different scenario is formed by sensitization with tetracene; that is, the generation of a single triplet excitation. This triplet is characterized in the transient experiments with tetracene by an absorption feature at wavelengths longer than 600 nm, which is close to that predicted theoretically at 689 nm ($1^3B_u \rightarrow 1^3A_g$ (Supporting Information Figure S5). The triplet lifetime of 111 μs measured in the sensitization experiment is in agreement with its single triplet character in contrast to the shorter lifetime for the two-triplet species.

In conclusion, a quinoidal bithiophene, QOT2, has been shown to be a very promising system for intramolecular singlet exciton fission with an outstanding efficiency of ~180%. This SEF quantum yield is among the largest found for organic molecules featuring SEF and, to the best of our knowledge, by far the greatest one for intramolecular SEF in small molecules. All critical parameters required for efficient SEF seems to coincide in QOT2: (i) its electronic structure which provides the $^1(T_1T_1)$ character to the key multiexciton 2^1A_g singlet electronic state; (ii) essentially planar geometry of the ground state associated with quinoid structure acquires substantial distortions in more aromatic excited state that help to accommodate two triplets on one molecule; (iii) the biradicaloid character expressed in the relevant excited states, which plays an important role in near optimal energy level arrangement for ultraefficient SEF on a subpicosecond time scale; and (iv) the high photostability provided by the thiophene stabilization of the oligoene path. Ultrafast time-resolved and integrated triplet accumulation photoinduced absorption experiments as well as time-resolved singlet fluorescence experiments, supported by CASPT2 and RAS-2SF calculations, all confirmed the occurrence of an ultrafast and efficient *intramolecular* singlet fission process in QOT2. This study on QOT2 will surely stimulate the search for new organic dye materials with focus on the challenging and elusive intramolecular singlet fission in small molecules, which up to now has been considered to be highly unlikely to exist.

■ EXPERIMENTAL METHODS

QOT synthesis has been reported previously.[22] For spectroscopic measurements on QOT2 solutions, the QOT2 was dissolved in THF unless otherwise noted. We have examined the transmission of the dimer (QOT2) solution in THF at 890 nm under constant illumination with the femtosecond pulse train beam at 445 nm. The 890 nm light beam has been produced by tunable Mai Tai laser system (Spectra Physics) delivering 130 fs pulses at repetition rate of ~80 MHz. The

second harmonic of this beam (445 nm, 2.79 eV) with an average power up to 80 mW has been produced in BBO crystal and used for excitation of the sample, whereas a small fraction of the fundamental beam (<1 mW) has served to probe the transmission at 890 nm where the linear absorption of QOT2 is negligible. A variable density neutral filter has been used to adjust excitation power at the sample. The laser beam has been focused on the sample cell using the lens with 127 mm focal length. Pure THF sample has been used as a reference in all experiments. A calibrated photodiode was used to measure the incident power. The transmitted power has been measured with a wide aperture power meter to avoid any contribution of the thermal lensing effect. Flash photolysis experiments were performed using nanosecond excitation from the Vibrant LD 355 II Nd:YAG/OPO system (OPOTEK) operating at 10 Hz. The transient absorption data were collected with an LP920 laser flash photolysis system (Edinburgh Instruments). The samples were degassed by argon prior to flash photolysis experiments. Femtosecond two-color pump–probe experiments on the dimer QOT2 were carried out using low noise, cavity-dumped Ti-Sapphire femtosecond oscillator. Excitation occurred at 415 nm, and the probe pulse wavelength was 830 nm. Pump pulse energy did not exceed 0.5 nJ at repetition rate ~39 kHz. Instrument response function duration for the two-color pump–probe configuration was ~100 fs. The experimental setup has been described in detail elsewhere.[50,51]

Time-correlated single photon counting (~1 ns resolution) was performed using the Ti:sapphire cavity dumped laser described above as an excitation source. Pulse repetition rate was set at 755 kHz in these experiments. Average pulse energy was ~13 nJ. A BBO crystal converts the 840 nm pulsed light into 420 nm excitation pulses. The fluorescence from the sample was collected at a right angle of excitation. Time resolution was created by using a time to amplitude converter (TAC), a linear ramp generator in the TimeHarp 200 (PicoQuant) detection card. Femtosecond time-resolved fluorescence measurements were carried out using fluorescence upconversion system with excitation provided by a frequency-doubled light from a mode-locked Ti-sapphire laser (Tsunami, Spectra-Physics) at 800 nm. Fluorescence emitted from the sample was up-converted in a nonlinear crystal of β-barium borate using a pump beam at 800 nm, which first passed through a variable delay line. Instrument response function (IRF, ~250 fs, fwhm) was measured using Raman scattering from water. Spectral resolution was achieved by using a monochromator and photomultiplier tube. More details of the upconversion setup are provided elsewhere.[51] The procedures and details of the theoretical studies are presented in the Supporting Information.

ASSOCIATED CONTENT

Ⓢ Supporting Information

Sensitization spectra and kinetics, induced absorption solvent viscosity dependence, singlet–triplet conversion yield calculations, computational details, RAS-2SF energy profiles, absorption spectrum concentration dependence, fluorescence magnetic field dependence. This material is available free of charge via the Internet at http://pubs.acs.org

AUTHOR INFORMATION

Corresponding Authors
*E-mail: tgoodson@umich.edu.
*E-mail: casado@uma.es.

Notes
The authors declare no competing financial interest.

REFERENCES

(1) Singh, S.; Jones, W. J.; Siebrand, W.; Stoicheff, B. P.; Schnider, W. G. Laser Generation of Excitons and Fluorescence in Anthracene Crystals. *J. Chem. Phys.* **1965**, *42*, 330–343.

(2) Congreve, D. N.; et al. External Quantum Efficiency Above 100% in a Singlet-Exciton-Fission-Based Organic Photovoltaic Cell. *Science* **2013**, *340*, 334–337.

(3) Chan, W.-L.; et al. Observing the Multiexciton State in Singlet fission and Ensuing Ultrafast Multielectron Transfer. *Science* **2011**, *334*, 1541–1545.

(4) Ehrler, B.; et al. *In situ* Measurement of Exciton Energy in Hybrid Singlet-Fission Solar Cells. *Nat. Commun.* **2012**, *3*, 1019.

(5) Zimmerman, P. M.; Zhang, Z.; Musgrave, C. B. Singlet Fission in Pentacene through Multi-exciton Quantum States. *Nat. Chem.* **2010**, *2*, 648–652.

(6) Smith, M. B.; Michl, J. Siglet Fission. *Chem. Rev.* **2010**, *110*, 6891–6936.

(7) Paci, I.; et al. Singlet Fission for Dye-Sensitized Solar Cells: Can a Suitable Sensitizer Be Found? *J. Am. Chem. Soc.* **2006**, *128*, 16546–16553.

(8) Geacintov, N.; Pope, M.; Fogel, F. Effect of Magnetic Field on the Fluorescence of Tetracene Crystals: Exciton Fission. *Phys. Rev. Lett.* **1969**, *22*, 593–596.

(9) Burdett, J. J.; Bardeen, C. J. Quantum Beats in Crystalline Tetracene Delayed Fluorescence Due to Triplet Pair Coherences Produced by Direct Singlet Fission. *J. Am. Chem. Soc.* **2012**, *134*, 8597–8607.

(10) Lanzani, G.; et al. Triplet-Exciton Generation Mechanism in a New Soluble (Red-Phase) Polydiacetylene. *Phys. Rev. Lett.* **2001**, *87*, 187402.

(11) Huynh, U.; Basel, T.; Xu, T.; Lu, L.; Zheng, T.; Yu, L.; Vardeny, V. Optical Properties of Low Bandgap Copolymer PTB7 for Organic Photovoltaic Applications. *Proc. SPIE* **2014**, *9165*, 91650Z.

(12) Busby, E.; Xia, J.; Wu, Q.; Low, J. Z.; Song, R.; Miller, J. R.; Zhu, X.-Y.; Campos, L. M.; Sfeir, M. Y. A Design Strategy for Intramolecular Singlet Fission Mediated by Charge-transfer States in Donor-Acceptor Organic Materials. *Nat. Mater.* **2015**, DOI: 10.1038/nmat4175.

(13) Gradinaru, C. C.; et al. An Unusual Pathway of Excitation Energy Deactivation in Carotenoids: Singlet-to-Triplet Conversion on an Ultrafast Timescale in a Photosynthetic Antenna. *Proc. Natl. Acad. Sci. U.S.A.* **2001**, *98*, 2364–2369.

(14) Polivka, T.; et al. Femtosecond Carotenoid to Retinal Energy Transfer in Xanthorhodopsin. *Biophys. J.* **2009**, *96*, 2268–2277.

(15) Wang, C.; Tauber, M. J. High-Yield Singlet Fission in a Zeaxanthin Aggregate Observed by Picosecond Resonance Raman Spectroscopy. *J. Am. Chem. Soc.* **2010**, *132*, 13988–13991.

(16) Müller, A. M.; Avlasevich, Y. S.; Müllen, K.; Bardeen, C. J. Evidence for Exciton Fission and Fusion in a Covalently Linked Tetracene Dimer. *Chem. Phys. Lett.* **2006**, *421*, 518–522.

(17) Michl, J.; et al. Toward Singlet Fission for Excitonic Solar Cells. *Proc. SPIE* **2007**, *6656*, 66560E.

(18) Johnson, J. C.; et al. Toward Designed Singlet Fission: Solution Photophysics of Two Indirectly Coupled Covalent Dimers of 1,3-Diphenylisobenzofuran. *J. Phys. Chem. B* **2013**, *117*, 4680−4695.

(19) Nozik, A. Nanoscience and Nanostructures for Photovoltaics and Solar Fuels. *Nano Lett.* **2010**, *10*, 2735−2741.

(20) Wang, Z.; Kobayashi, T. Electronic Relaxation and Vibrational Dynamics in a Thiophene Oligomer Studied Under the Same Experimental Condition with Sub-5 fs Laser. *New J. Phys.* **2008**, *10*, 123021.

(21) Raymond, J. E.; Casado, J.; Lopez Navarrete, J. T.; Takimiya, K.; Goodson, T., III Two-Photon Mediated Three-Photon Fluorescence: Lessons from a Quinoidal Oligothiophene Dimer. *J. Phys. Chem. Lett.* **2011**, *2*, 2179−2183.

(22) Takahashi, T.; Matsuoka, K.; Takimiya, K.; Otsubo, T.; Aso, Y. Extensive Quinoidal Oligothiophenes with Dicyanomethylene Groups at Terminal Positions as Highly Amphoteric Redox Molecules. *J. Am. Chem. Soc.* **2005**, *127*, 8928−8929.

(23) Casado, J.; Lopez Navarrete, J. T. The Longest Quinoidal Oligothiophene: A Raman Story. *Chem. Rec.* **2011**, *11*, 45−53.

(24) Ortiz, R. P.; et al. Quinoidal Oligothiophenes: Towards Biradical Ground-State Species. *Chem.—Eur. J.* **2010**, *16*, 470−484.

(25) Ortiz, R. P.; et al. On the Biradicaloid Nature of Long Quinoidal Oligothiophenes: Experimental Evidence Guided by Theoretical Studies. *Angew. Chem., Int. Ed. Engl.* **2007**, *46*, 9057−9061.

(26) Casado, J.; Ponce Ortiz, R.; López Navarrete, J. T. Quinoidal Oligothiophenes: New Properties behind an Unconventional Electronic Structure. *Chem. Soc. Rev.* **2012**, *41*, 5672−5686.

(27) Gonzalez, S. R.; Ie, Y.; Aso, Y.; Lopez Navarrete, J. T.; Casado, J. The Frontiers of Quinoidal Stability in Long Oligothiophenes: Raman Spectra of Dicationic Polaron Pairs. *J. Am. Chem. Soc.* **2011**, *133*, 16350−16353.

(28) Di Motta, S.; Negri, F.; Fazzi, D.; Castiglioni, C.; Canesi, E. V. The Biradicaloid and Polyenic character of Quinoidal Oligothiophenes Revealed by the Presence a Low Lying Double-Exciton State. *J. Phys. Chem. Lett.* **2011**, *1*, 3334−3339.

(29) Bonaicic-Koutecky, V.; Koutecky, J.; Michl, J. A Neutral and Charged Biradicals, Zwitterions, Funnels in S$_1$ and Proton Translocation:Their Role in Photochemistry, Photophysics, and Vision. *Angew. Chem., Int. Ed.* **1987**, *26*, 170−189.

(30) Minami, T.; Nakano, T. Diradical Character View of Singlet Fission. *J. Phys. Chem. Lett.* **2011**, *3*, 145−150.

(31) Trinh, M. T.; Zhong, Y.; Chen, Q.; Schiros, T.; Jockusch, S.; Sfeir, M. Y.; Steigerwald, M.; Nuckolls, C.; Zhu, X. Intra- to Intermolecular Singlet Fission. *J. Phys. Chem. C* **2014**, *119*, 1312−1319.

(32) Monahan, N.; Zhu, X.-Y. Charge-Transfer-Mediated Singlet Fission. *Annu. Rev. Phys. Chem.* **2015**, *66*, 601−618.

(33) Izumi, T.; Kobashi, S.; Takimiya, K.; Aso, Y.; Otsubo, T. Synthesis and Spectroscopic Properties of a Series of α-Blocked Long Oligothiophenes up to the 96-mer: Revaluation of Effective Conjugation Length. *J. Am. Chem. Soc.* **2003**, *125*, 5286−5287.

(34) Walker, B. J.; Musser, A. J.; Beljonne, D.; Friend, R. H. Singlet Exciton Fission in Solution. *Nat. Chem.* **2013**, *5*, 1019−1024.

(35) Chan, W.-L.; et al. The Quantum Coherent Mechanism for Singlet Fission: Experiment and Theory. *Acc. Chem. Res.* **2013**, *46*, 1321−1329.

(36) Ryasnyanskiy, A.; Biaggio, I. Triplet Exciton Dynamics in Rubrene Single Crystals. *Phys.Rev. B* **2011**, *84*, 193203.

(37) Roberts, S. T.; et al. Efficient Singlet Fission Discovered in a Disordered Acene Film. *J. Am. Chem. Soc.* **2012**, *134*, 6388−6400.

(38) Müller, A. M.; Avlasevich, Y. S.; Schoeller, W. W.; Müllen, K.; Bardeen, C. G. Exciton Fission and Fussion in Bis(tetracene) Molecules with Different Covalent Linker Structures. *J. Am. Chem. Soc.* **2007**, *129*, 14240−14250.

(39) Serrano-Andres, L.; Merchan, M. Quantum Chemistry of the Excited State: 2005 overview. *J. Mol. Struct.: THEOCHEM* **2005**, *729*, 99−108.

(40) Serrano-Andrés, L. Serrano-Pérez, J. J. In *Handbook of Computational Chemistry*; Leszczynski, J., Ed.; Springer: Netherlands, 2012; Ch. 14, pp 483−560.

(41) Shulten, K.; Karplus, M. On the Origin of a Low-Lying Forbidden Transition in Polyenes and Related Molecules. *Chem. Phys. Lett.* **1972**, *14*, 305−309.

(42) Tavan, P.; Schulten, K. Electronic Excitations in Finite and Infinite Polyenes. *Phys. Rev. B* **1987**, *36*, 4337−4358.

(43) Casanova, D.; Head-Gordon, M. Restricted Active Space Spin-flip Configuration Interaction Approach: Theory, Implementation and Examples. *Phys. Chem. Chem. Phys.* **2009**, *11*, 9779−9790.

(44) Casanova, D. Efficient Implementation of Restricted Active Space Configuration Interaction with the Hole and Particle Approximation. *J. Comput. Chem.* **2013**, *34*, 720−730.

(45) Bell, F.; Casanova, D.; Head-Gordon, M. Theoretical Study of Substituted PBPB Dimers: Structural Analysis, Tetraradical Character, and Excited States. *J. Am. Chem. Soc.* **2010**, *132*, 11314−11322.

(46) Zimmerman, P. M.; Bell, F.; Casanova, D.; Head-Gordon, M. Mechanism for Singlet Fission in Pentacene and Tetracene: From Single Exciton to Two Triplets. *J. Am. Chem. Soc.* **2011**, *133*, 19944−19952.

(47) Zimmerman, P. M.; Musgrave, C. B.; Head-Gordon, M. A Correlated Electron View of Singlet Fission. *Acc. Chem. Res.* **2013**, *46*, 1339−1347.

(48) Tayebjee, M. J. Y.; Clady, R. G. C. R.; Schmidt, T. W. The Exciton Dynamics in Tetracene Thin Film. *Phys. Chem. Chem. Phys.* **2013**, *15*, 14797−14805.

(49) Wang, Z.; Otsubo, T.; Kobayashi, T. Chirped Modulation of Molecular Vibration in Quinoidal Thiophene after Sub-5 fs Excitation. *Chem. Phys. Lett.* **2006**, *430*, 45−50.

(50) Donehue, J. E.; Varnavski, O. P.; Cemborski, R.; Iyoda, M.; Goodson, T., III Probing Coherence in Synthetic Cyclic Light-Harvesting Pigments. *J. Am. Chem. Soc.* **2011**, *133*, 4819−4828.

(51) Varnavski, O.; Yan, X.; Mongin, O.; Blanchard-Desce, M.; Goodson, T., III Strongly Interacting Organic Conjugated Dendrimers with Enhanced Two-Photon Absorption. *J. Phys. Chem. C* **2007**, *111*, 149−162.